

A dynamic model for the mutual constitution of individuals and events

JÜRGEN LERNER  †

Department of Computer and Information Science, University of Konstanz, 78457 Konstanz, Germany

†Corresponding author. Email: juergen.lerner@uni-konstanz.de

AND

ALESSANDRO LOMI

Faculty of Economics, University of the Italian Switzerland, Lugano 6900, Switzerland

Edited by: Matjaz Perc

[Received on 15 October 2021; editorial decision on 30 January 2022; accepted on 2 February 2022]

We argue and show that a recently derived class of relational hyperevent models (RHEM) may be adopted to extend the sociological concept of duality by linking it to empirical data containing information on the temporal order of events. We show how RHEMs may be specified to predict the likelihood that combinations of individuals of any size will jointly participate in future events, conditional on their history of participation in past events. We show, further, how RHEMs may support hypothesis testing about competing mechanisms driving participation in events. Finally, we show how RHEMs may be used to establish the location of the events that actually happened in the much larger space of all the possible events that could have happened, but did not. We illustrate the empirical value of RHEMs using a canonical dataset containing information on the participation of 18 women in 14 time-ordered events. We provide dynamic network visualizations to link empirical estimates of the model parameters to qualitative insight on the dynamics of the mutual constitution of individuals and events. While RHEMs are also applicable to large networks (e.g. coauthorship networks), using a small canonical dataset allows us to examine in greater detail the model's implications for each and every observed event and to identify the location of each event participant in the network of previous events. Scaling down our model to examine a small dataset affords a more detailed understanding of the link between quantitative model results expressed as parameter estimates, and the qualitative features of the original observations.

Keywords: duality of persons and groups; two-mode networks; hypergraphs; longitudinal network models; relational hyperevent models; Deep South.

1. Introduction

Broadly inspired by Georg Simmel's classic sociological imagery of intersecting social circles ('Die Kreuzung sozialer Kreise'), more recent research has emphasized the relation of mutual constitution linking individuals and events they attend—or groups in which they participate [1]. According to this view, individuals and events stand in a mutually constitutive relation: individual identities are defined by the intersection of the multiple events they attend. Dually, events are defined by the intersection of individuals attending them [2]. This intuition about the dual association between individuals and events was first formalized by Breiger [3] who extended and refined it in a number of subsequent contributions [4–8].

This concept of duality may be encountered in a surprising variety of empirical guises across diverse studies. Examples include participation in terrorist groups [9, 10], scientists and papers they coauthor

[11], members of venture capital syndicates and companies they invest in [12], scientific publications and keywords used to describe their content [13], software developers and problems ('bugs') they discover in software code [14] and Wikipedia editors and text they write [15]. However apparently diverse, all these examples involve 'events' bringing together individuals at specific points in time—with each observed event typically involving only a small subset of individuals drawn from a much larger population of potential participants who could have attended the event, but did not.

In this article, we contribute to this diverse literature broadly inspired by duality concepts by applying recently derived relational hyperevent models [16] to the analysis of mutual constitution of individuals and their attendance in time-stamped events. The model extends the applicability of duality concepts to relational event data by incorporating explicit dynamic elements in the form of a time-ordered sequence of events to which individual participate. This apparently obvious addition reveals the link between concepts of duality proposed by Breiger [3] and the mathematical representation of events as hyperedges connecting multiple actors simultaneously [16]. Building on the recently derived class of relational event models (REMs) for directed social processes [17, 18], the model posits that a list of relational hyperevents reveals which hyperedges of a hypergraph are more likely to experience joint events. The model locates observed hyperedges within the space of possible hyperevents that could have happened but did not. Hypergraphs are generalizations of graphs [19, 20]. In the latter each edge connects exactly two actors, while in the former a hyperedge may connect an arbitrary number of actors through one simultaneous event. Following [16, 21], we define a *relational hyperevent* as a hyperedge—comprising the set of event *participants*—with a time stamp specifying *when* the event took place. A variant of RHEM for directed hyperevents has been applied to model contact elicitation by infected persons in an analysis of virus-spreading networks [22].

The model adopted in this article significantly expands the analytical functionality and empirical applicability of available models for relational events [23]. More specifically, the RHEM contains at least three main elements of innovation distinguishing it from more established models of mutual constitution [4, 14], and from available models for relational events [17, 18, 24, 25]. First, RHEMs may be specified to predict the likelihood of all combinations of individuals ('groups') of any size to jointly participate in future events, conditional on their history of participation in past events. The new specification adds to existing models the possibility of formulating extra-dyadic predictions—that is, predictions about *clusters* of individuals simultaneously attending an event. Models are available that correct for the presence of multi-actor events deriving from multicast communication [24], that is, message events with multiple receivers—however, they do so by assuming independence of event rates on *dyads* linking the sender to each of the receivers, one by one. Moreover, available models to *control* for multicast interaction miss the opportunity for theoretical development that aims to *explain* multicast interaction by empirically testable hypotheses.

Second, RHEMs support hypothesis testing about competing mechanisms driving participation in events like, for example, varying popularity of individuals as event participants (preferential attachment), the preferential tendency of individuals to co-attend events with familiar alters (repeated joint participation), or the preferential tendency of individuals sharing a common alter to participate in the same future event (triadic closure). RHEMs not only afford prediction of clusters of actors simultaneously attending events but also help discriminating among underlying mechanisms that shape the composition of the clusters. Available approaches model simultaneous joint actions from or to multiple actors by creating fictitious (or 'virtual') aggregate actor nodes [18]. However useful, this approach precludes examination of the entire space of alternative actor sets that could have experienced events, but did not, thereby precluding examination of alternative mechanisms driving participation of multiple individuals in events.

Third, RHEMs may be used to describe the events that actually happened in relation to the space of all the possible events that could have happened, but did not (compare Section 3.5.2). To the best of our knowledge, no other statistical model for relational events is available that affords these analytical possibilities, and combine them into a single specification.

We test the empirical value of RHEMs on the canonical ‘Deep South’ dataset originally collected by Davis, Gardner and Gardner in the 1930’s [26], henceforward denoted as *DGG data*. This dataset containing information on participation of 18 women in 14 time-ordered events has been used extensively in the analysis of group structure [27]. The DGG dataset is ideal for our current purposes because it contains information on the timing of events which allows us to order in time the sequence of observed events. The DGG dataset has the further advantage of making the results we report in the empirical part of the article comparable, at least in principle, to the results produced by models for two-mode networks tested on the same data [9, 28].

Our choice of empirical illustration is only apparently idiosyncratic. In fact, not only the DGG dataset was used to illustrate the original duality idea [3], but it has also been recurrently used to test network-analytic models of group structure and processes [9, 27]. More importantly for our current purposes, the example reproduces at a small scale structural features of much larger datasets that have been analysed with RHEM [21]. The illustration we provide is functional to our objective to explore the qualitative insight that quantitative analysis may be able to support—an issue that is becoming increasingly crucial [29].

Our empirical analysis based on the DGG dataset provides the additional advantage of being fully reproducible (compare Section 4.1). Moreover, RHEM model results are complemented by descriptive analysis providing a unique link from the observed data—and the characteristics of events and their constituting participants—over to the final conclusions supported by empirically estimated RHEMs. This is a significant contribution over previous papers, for example, [16, 22], since network effects revealed by RHEM parameter tables are now transparently linked to the original empirical observations. In the Discussion section that concludes the article, we provide dynamic network visualizations that help to actually *see* the main qualitative implications of the empirical estimates of the model parameters, and link them to more general questions that RHEMs now make possible to ask.

2. Background and motivation

A radical implication of the duality principle proposed by Breiger [3] is that individuals *are* the groups they are members of and, dually, groups *are* the set of their members [2, p. 301]. The empirical range of phenomena standing in a similar relation of mutual constitution is very broad and covers, for example, organizational practices and cultural categories they create [30], organizations and projects they are involved in [31], technology and creative practices they afford [32], social relations and discursive practices they sustain [33] and organizations and audiences they engage, niches they occupy, and activities they organize [34–36]. Common examples of dual phenomena produced by mutually constitutive relations involving individuals include interlocking boards of directors [37, 38], social events co-attended by multiple participants [27], researchers co-authoring scientific papers [11], artists involved in multiple productions [39] and participants in peer-production projects engaging multiple problems [14, 40].

In all these diverse cases, the affiliation of ‘individuals’ to various ‘groups’ through jointly attended events or shared activities is often represented as a two-mode matrix—a rectangular array whose rows are indexed by the individuals and whose columns are indexed by groups [20]. A two-mode network has two sets of nodes, the set of actors and the set of groups, and edges in the actor-group network connect actors

to the groups they are members of [28, 41, 42]. Two-mode networks do *indirectly* provide information on the relation internal to the set of individuals, or the set of groups.

Two-mode networks are produced naturally by what [43] calls involvement of individuals in events [20, p. 291–294]. According to Wasserman and Faust, ‘*Common to all of these views is the idea that actors are brought together through their joint participation in social events*’ [20, p. 293].’ However, while the affiliation of individuals to (multiple) groups need not be associated with a specific time stamp [44], the involvement of individuals in (multiple) events occupies a specific position in a sequence of events ordered in time.

Two-mode actor–event networks can be represented by a hypergraph [20, 45, 46]. A hypergraph has a set of nodes, representing the actors, and a set of hyperedges, representing the events. In contrast to edges in ordinary graphs which connect exactly two nodes, a hyperedge can contain any number of nodes and, thus, a single hyperedge can represent an entire event by containing all of its participants. Unlike edges in networks connecting individuals to groups, hyperedges generate multiple simultaneous two-mode edges. This property of hypergraphs is essential to the unique ability of RHEM to represent simultaneous participation of multiple individuals in the same event.

Our article is based on the claim that prior formalizations of duality—including statistical models for dynamic two-mode networks, for example, [47, 48]—have overlooked this crucial distinction in the *dynamics* of actor–event networks. In some settings, event nodes exist over extended periods of time during which actors can individually connect to, or disconnect from events. This type of dynamics applies, for instance, to two-mode networks in which event nodes represent company boards where directors can individually join or leave [37, 38], or to networks in which event nodes represent organizational problems that organizational participants can tackle individually at different points in time [14]. In this article, we are concerned with a fundamentally different type of two-mode network dynamics in which event nodes represent ‘one-time events’ connecting all of their participants in one simultaneous multi-actor event. This type of dynamics is typical of networks of actors co-attending social events [26, 27], co-authors publishing joint scientific papers [11] and people attending meetings recorded in contact diaries [16]. In these settings, event nodes can be associated with one single point in time at which all participants are linked in one simultaneous composite multi-actor event, or *hyperevent*.

The simultaneity of hyperedges confronts us with the need to adopt a recently defined model, thereby extending Breiger’s concept of duality to incorporate dynamic elements inherent in the notion of ‘events’ as unique *social foci* explicitly situated in time (and, obviously, space) [49, 50]. RHEMs [16] can model the probability to jointly experience an event of every possible groups of actors—whatever its size. RHEMs may be also specified to test competing hypotheses about the mechanisms that shape co-attendance at events. Finally, RHEMs can help locate hyperevents that are actually observed in the space of all possible hyperedges that could have experienced common events but did not. We will further demonstrate that a combination of inferential and descriptive techniques enables a seamless connection from the observed data—and the characteristics of events and their constituting participants—to the final inferential conclusions produced by RHEM.

3. Relational hyperevent models

3.1 Two-mode networks and hypergraphs

A *relational hyperevent* $e = (t_e, h_e)$ is a pair consisting of a time stamp t_e (the time of the event) and a set of participants $h_e \subseteq V$ which is a subset of a given sample of actors V [16, 21]. A list of relational hyperevents $E = (e_1, \dots, e_N)$ gives rise to two equivalent networks: a two-mode actor–event network and

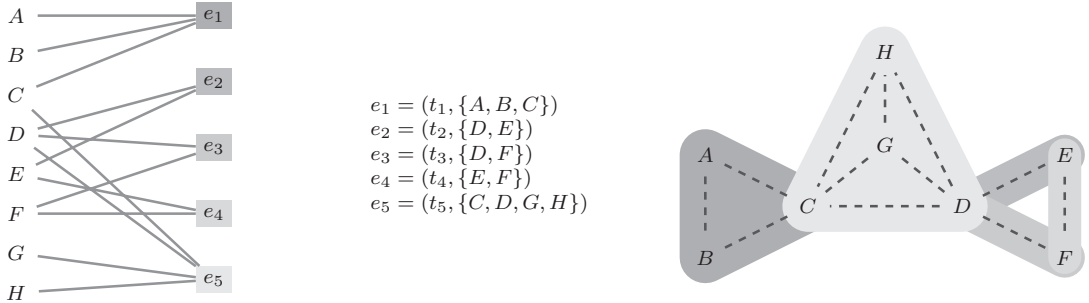


FIG. 1. Illustration of hyperevents and the associated two-mode network and hypergraph, reproduced from [16]. In the *middle* is a list of five hyperevents $e_i = (t_i, h_i)$, $i = 1, \dots, 5$ occurring at event times t_i jointly attended by participants from $h_i \subseteq \{A, \dots, H\}$. On the *left* is the two-mode actor–event network representing the given sequence of hyperevents. On the *right* is the hypergraph representation of the given sequence of hyperevents, each giving rise to a hyperedge displayed as a grey-shaded area enclosing the event participants. Edges in the one-mode projection to the set of actors are given by dashed lines.

a hypergraph [19, 20, 45, 46]; see Fig. 1 for a stylized example. In the two-mode network, the nodes in the first mode (the ‘actor’ mode) are the set of actors V , the nodes in the second mode (the ‘event’ mode) are the set of events E , and an actor $v \in V$ is connected to an event $e \in E$ via an edge in the two-mode graph if v is contained in the participant list of e , that is, if $v \in h_e$. The *hypergraph* [19] resulting from a list of relational hyperevents is a pair $G = (V, H)$ in which V is the set of actors (the nodes of the hypergraph) and H is a set of *hyperedges*, that is, $H = \{h_e ; e \in E\}$. Each element $h_e \in H$ is the set $h_e \subseteq V$ of participants of the event $e = (t_e, h_e)$. Hypergraphs are generalizations of graphs, since in the latter each edge connects exactly two actors, while in the former a hyperedge can connect any number of actors in one simultaneous event.

In general, it is possible that the same set of actors $h \subseteq V$ experiences more than one joint event—typically at different points in time. Thus, a list of relational hyperevents gives rise to a multi-hypergraph in which hyperedges have *multiplicities*—positive integers giving the number of times that the participants of the hyperedge co-attend an event—and in which each hyperedge is associated with the list of time points at which these events take place. In the two-mode representation, multiple events on the same set of participants give rise to structurally equivalent event nodes [20], that is, event nodes that are adjacent to the same set of actor nodes.

Two-mode graphs can be projected to the set of actors [28]. Edges in these one-mode projections connect two actors if there is at least one event in which both participate. In contrast to hypergraphs, which are equivalent representations of two-mode networks, one-mode projections involve a loss of information. For instance, three actors that form a closed triangle in the one-mode projection might result from a single event in which all three participated—or the triangle might result from three different events in each of which just two of the three actors participated pairwise; compare the two triads $\{A, B, C\}$ vs. $\{D, E, F\}$ given in Fig. 1. Moreover, one-mode projections induce structural artefacts, such as high local density and an abundance of closed triangles. For instance, a single hyperevent with 10 participants gives rise to 45 ties, forming a clique of size 10 and 120 closed triangles.

3.2 Limitations of related models

Hypergraphs can be examined through dedicated inferential network models for two-mode networks. Examples include models for ‘relational states’ [14, 47, 48, 51–54], and models for ‘relational events’

[18, 38, 55, 56]. However, in contrast to RHEM, these models cannot cope with the dynamics of relational hyperevent networks sketched above where events involve simultaneous interaction among a set of actors of any size.¹

Models based on stochastic actor-oriented models (SAOM) [47, 48, 52] or temporal exponential random graph models (TERGM) [53, 54] typically condition on the observed set of nodes—that is, in a two-mode scenario, the set of actor nodes and the set of event nodes—and specify the joint probability of tie variables indicating which actor nodes are connected to which event nodes in a given time step. This representation does not fit well situations in which one class of nodes represent one-time events such as social meetings that can be attended by a set of actors of any size only once. If the time granularity of the observation scheme is sufficiently high and event times are unique, then in each time step there is exactly one new event node added to the network and the ‘free’ tie variables (i.e. those dyads whose edge probability has to be modelled in the given time step) are only those dyads connecting actors to the single newly added node. Edges indicating attendance of past events can no longer be changed since an actor who has attended a specific event will always have attended that event and an actor who has not attended a specific event does not have the possibility to join later. In other words, available dynamic models for networks do not fit well situations where events are defined in terms of ephemeral (i.e. non-repeatable) social foci [50]. Aggregating events over longer time intervals, or ‘time slices’, tends to be associated with information loss since the order of events within any given interval cannot be recovered.

Existing REM for two-mode networks [18, 38, 55, 56] can handle the fine-grained dynamics of event network data, but typically specify dyadic event rates connecting one source node to one target node. Treating multi-actor events as collections of independent dyadic events involves the analytically convenient, but empirically implausible assumption that multiple dyadic relations between the single sender and the set of simultaneous receivers are independent.

Butts [18] proposes the creation of virtual nodes representing sets of actors to deal with situations of multiple senders or receivers. This solution may be feasible to deal with a small number of predefined actor sets—such as the set of all actors to model ‘broadcast’ events [61, 62]—but it becomes increasingly less practical as the set of potential actors that need to be considered expands. This is the case because the space of all sets of actors that could potentially constitute the participant list of the next event increases exponentially in the number of actors.

The hyperedge event model of Kim *et al.* [63] can specify the probability that one source node sends an event directed at any number of receivers (‘multicast communication’), but it does so by specifying dyadic event intensities (i.e. the rate that one source sends an event to one receiver) and constructing larger receiver sets from these dyadic intensities. This is less general than in RHEM [16] which can specify intensities associated with all subsets of nodes of any size. Along similar lines, Perry and Wolfe [24] recognize the importance of multicast interaction (i.e. simultaneous interaction between one sender and multiple receivers) but the solution they provide hinges on the assumption that the sending rate to the set of multiple receivers is the product of the corresponding dyadic rates. In other words, these authors assume that the dyads connecting the sender to the various receivers are independent, an assumption that is particularly problematic in the case of multicast interaction.

¹ In the discussion that follows, we will not be referring to the problem of ‘tied times’—simultaneity of events induced by observation schemes whose low temporal resolution is insufficient to capture the exact timing of individual events [57]. When the number of ‘ties’ (simultaneous events) is small, a number of statistical procedures are available to make unbiased estimation possible [58–60]. We will be focusing on the cases in which the simultaneity of events is a *structural* feature of the data, like, for example data produced by contact diaries [16], or data produced by joint participation of individuals to various kinds of groups, decision situations or social events.

The conclusion of this discussion seems to be that many existing REMs do not have a good way to deal with multicast interaction that commonly characterizes dual phenomena such as, for example, participation of individuals in meetings with clear starting and ending times. Previous models may apply to scenarios in which event nodes exist over extended periods in time (such as boards of directors or organizational problems) during which actors can connect to, disconnect from, or engage in these event nodes individually at different points in time. However, established statistical network models do not apply to the common situation in which event nodes represent one-time events (such as social events, or gatherings) associated with a single point (or interval) in time during which all participants interact simultaneously. We therefore adopt the RHEM framework proposed in [16] to model these situations.

3.3 Modelling relational hyperevents

RHEMs are a general model framework for sequences of time-stamped multi-actor events. RHEM can test hypotheses explaining the propensity of groups to co-participate in joint events by previous events and/or by given covariates. The description of the model framework closely follows [16]. The dependent variable that is modelled by relational hyperevent models (RHEM) is the time-varying *event intensity* $\lambda(t; h)$ associated with any set of actors $h \subseteq V$ that could potentially experience a joint event at time t . Informally, the event intensity is the expected number of events with set of participants equal to h in a time-interval of unit length. More formally [64]:

$$\lambda(t; h) = \lim_{\Delta t \rightarrow 0} \frac{\mathbb{E}(|\{e \in E ; h_e = h \wedge t \leq t_e < t + \Delta t\}|)}{\Delta t}.$$

Following the Cox proportional hazard (CoxPH) model [65, 66], the intensity function $\lambda(t; h)$ is decomposed into a non-parametric, time-varying global baseline rate $\lambda_0(t)$ and a parametric factor $\lambda_1(t; h; \theta)$ revealing the *hazard ratio*, that is, the factor by which the intensity associated with hyperedge h is larger or smaller than the baseline rate. The relative rate $\lambda_1(t; h; \theta)$ is specified as a function of hyperedge statistics $s(t; h; E) = (s_1(t; h; E), \dots, s_k(t; h; E)) \in \mathbb{R}^k$, which are the explanatory variables for the intensity of hyperedge h at time t and are functions of the past events $E_{<t} = \{e \in E ; t_e < t\}$, and associated parameters $\theta = (\theta_1, \dots, \theta_k) \in \mathbb{R}^k$:

$$\lambda_1(t; h; \theta) = \exp \left(\sum_{i=1}^k \theta_i s_i(t; h; E) \right). \quad (3.1)$$

For each event $e = (t_e, h_e)$ let $R_{t_e} \subseteq \mathcal{P}(V)$, with $h_e \in R_{t_e}$, denote a suitable definition of the *risk set*—containing *possible participant lists* for an event at time t_e that we want to compare with the actually observed participant list h_e . The CoxPH model yields a partial likelihood function for observing the sequence of events $E = (e_1, \dots, e_N)$ given by

$$L(\theta) = \prod_{e \in E} \frac{\lambda_1(t_e; h_e; \theta)}{\sum_{h \in R_{t_e}} \lambda_1(t_e; h; \theta)} \quad (3.2)$$

and parameters θ are estimated to maximize this likelihood.

A generally applicable definition is to let the risk sets contain all subsets of a given sample of actors V , that is, $R_{t_e} = \mathcal{P}(V)$, which we denote in the following as *unconstrained risk sets*. However, this approach has the drawback that the number of sets of actors of size k largely depends on the relation

of k to n . In the empirical co-attendance network that we analyse in Section 4, we have a sample of $n = |V| = 18$ actors, implying, for instance, $\binom{18}{2} = 153$ possible participant lists containing exactly two actors, but $\binom{18}{9} = 48\,620$ participant lists of size $k = 9$. In general, unconstrained risk sets contain an over-representation of participant lists whose size is about half the total number of actors—which is unrealistic in many empirical networks. Thus, in the empirical analysis given in Section 4, we follow the recommendation of [16] and consider *conditional-size* RHEM whose risk sets contain all participant lists of the same size as the observed event, that is, $R_e = \{h \subseteq V ; |h| = |h_e|\}$.

Lerner *et al.* [16, 21] proposed to speed up the computation of the likelihood function through nested case-control sampling [67, 68] in which only a random sample of fixed size from the risk set at the event times is included. Indeed, the size of the risk set (i.e. the number of sets of actors that could potentially experience joint events) grows exponentially in the number of actors. Case-control sampling has been successfully applied to estimate parameters of dyadic REM for large networks [56] and to RHEM estimated on hypergraphs with hundreds of thousands of nodes [21]. However, in the empirical application in this article, we consider a relatively small co-attendance network of 14 events attended in total by 18 actors—yielding a maximal risk set size of $2^{18} = 262,144$ (or up to $\binom{18}{9} = 48\,620$ for size-constrained risk sets)—which makes sampling superfluous. In fact, given such a small empirical dataset, we prefer to use all available information and avoid adding any measure of sampling error.

3.4 Effects in relational hyperevent networks

RHEMs are specified through hyperedge statistics describing how groups of actors—both, those actually experiencing the next event, and those who could have potentially experienced the next event—are embedded into the network of past events. These hyperedge statistics operationalize hypothetical network effects in dynamic co-attendance networks and the estimated parameters associated with hyperedge statistics yield rigorous statistical tests for these hypotheses. To keep the exposition intuitive and general, we review only relatively simple and generally applicable statistics.

A core behavioural assumption is that actors remember prior joint events they have attended—so that past events can have an influence on the propensity to experience future joint events with the identical or an overlapping participant list. To provide a concrete example, Event 3 on March 2nd in our empirical data (compare Fig. 2) is attended by the three participants Evelyn, Laura and Theresa. We assume that each of these actors—when deciding whether to attend Event 3 together with the two others—remembers that she has already co-participated with them in Event 2 on February 25th. Thus, the past Event 2 signals a preference for co-attendance which, in turn, increases the likelihood that these three actors constitute (part of) the participant list of a future event—such as Event 3.

Past joint events are quantified through the *hyperedge degree* that counts the number of prior events co-attended by all members of a given group of actors. Formally, the hyperedge degree of $h \subseteq V$ at time t , denoted by $hy.deg(t; h; E)$, is defined by

$$hy.deg(t; h; E) = |\{e \in E ; h \subseteq h_e \wedge t_e < t\}|.$$

Discussing some special cases, the hyperedge degree of a single-actor set $h = \{v\}$ at time t is the number of events in which actor v participated previous to t . Thus, the hyperedge degree of a single-actor set is the ‘hypergraph version’ of the usual degree of nodes in ordinary graphs (recall that the degree of a node v in a graph is the number of edges incident to v). Going beyond the notion of degree in ordinary graphs, the hyperedge degree of a two-actor set $h = \{u, v\}$ is the number of past events that are jointly attended

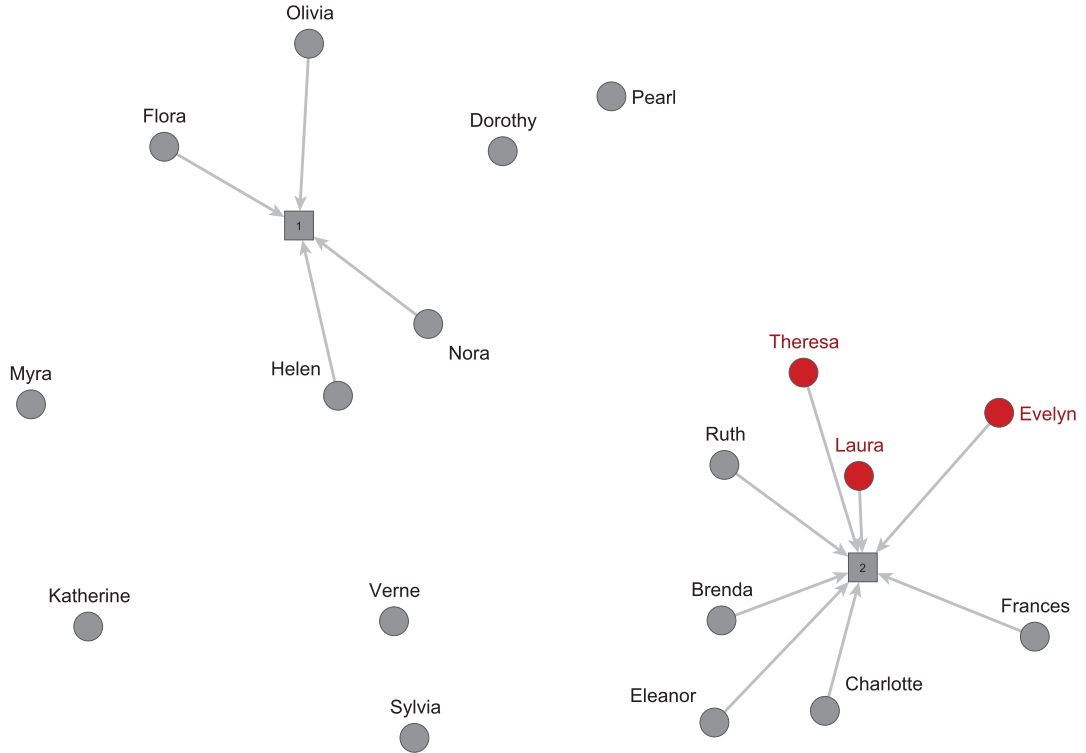


FIG. 2. DGG network shortly before Event 3 whose participants are displayed in red. Events are displayed as square-shaped nodes, participants are displayed as circles, and participants are connected to the events they attend by directed edges. Participants of Event 3 are a subset of those of Event 2.

by u and v . In general, the hyperedge degree of a set of actors $h \subseteq V$ is the number of past events that are co-attended by all actors in h —possibly together with a varying set of other participants.

3.4.1 Partial repetition. A common—and very plausible—effect in dynamic co-attendance networks captures the tendency that a future joint event on a hyperedge h becomes more likely if some of the members of h have previously co-attended common events. To provide more interpretable network effects, it is convenient to distinguish the order of subsets that repeatedly co-attend events. For instance, subset repetition of order one considers the number of prior events in which any of the members of h participated—alone or jointly with varying other participants. Thus, subset repetition of order one implements a *preferential attachment* effect [69], predicting that actors who were more popular event attendees in the past will accumulate future events at a higher rate. Operationalizing a different network effect, subset repetition of order two considers the number of prior *joint* events of pairs of members of h . Thus, subset repetition of order two operationalizes a *dyadic familiarity* effect, predicting that a group of actors h is more likely to experience a future joint event if pairs of members of h have a history of prior shared activity. In general, and more formally, for a given integer $p \geq 1$, *subset repetition of order p*, denoted

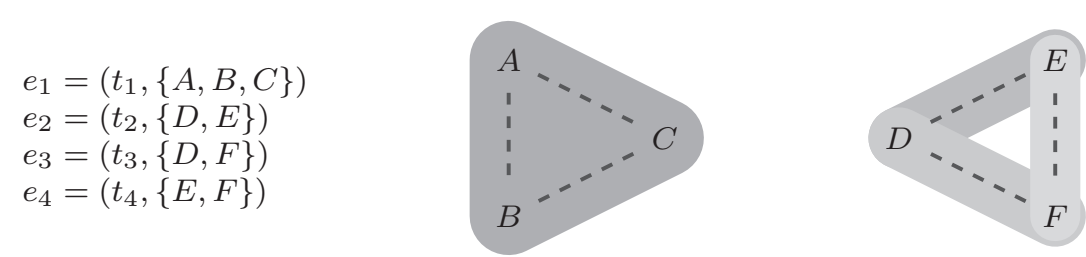


FIG. 3. Illustrating subset repetition of various orders on some of the hyperevents from Fig. 1. The hyperedge $\{A, B, C\}$ has subset repetition of order one, two and three all equal to one since each individual has participated in one event, each dyad has co-participated in one event, and the whole triad has also co-participated in one joint event. The hyperedge $\{D, E, F\}$ has subset repetition of order one equal to two (each actor individually participated in two events), subset repetition of order two is equal to one (one joint event for each dyad), and subset repetition of order three is zero (no joint event for the whole triad).

by $\text{sub.rep}^{(p)}(t; h; E)$, is defined by

$$\text{sub.rep}^{(p)}(t; h; E) = \sum_{h' \in \binom{h}{p}} \frac{\text{hy.deg}(t; h'; E)}{\binom{|h|}{p}},$$

where $\binom{|h|}{p}$ is the binomial coefficient (i.e. the number of subsets of size p of a set with $|h|$ elements) and $\binom{h}{p}$ is a symbolic notation for the set of subsets of size p of h :

$$\binom{h}{p} = \{h' \subseteq h ; |h'| = p\}.$$

Subset repetition of various orders is illustrated in Fig. 3. In the empirical example reported in this article we denote subset repetition of order one by ‘individual activity’, $\text{sub.rep}^{(2)}$ by ‘dyadic shared activity’, and $\text{sub.rep}^{(3)}$ by ‘triadic shared activity’.

3.4.2 Triadic closure. A different type of effects generally observed in social networks is related to triadic closure [70]. Given that two actors have previously interacted with at least one common third actor, the research question is whether these two actors are more or less likely to interact directly with each other. It is possible to devise theoretical arguments that would be consistent with an effect in either direction. Balance theory [71] predicts that actors cognitively organize triadic relations in a balanced way: if two actors interacted with a common third—and given that interaction can be considered as revealing a ‘positive’ relation—then the two actors that share the common acquaintance are predicted to be more likely to interact themselves. This line of reasoning would support predictions of a tendency in favour of triadic closure (i.e. a positive effect of parameters associated with closure statistics). In contrast, according to structural holes arguments [72] actors occupying brokerage positions—such as the third actor mediating between the two others—gain competitive advantage and/or, from the other point of view, the two other actors compete for access to the broker. This line of reasoning would support predictions of a tendency against triadic closure (i.e. a negative effect of the parameters associated with closure statistics).

Thus, whether we expect a tendency for or against triadic closure depends on the nature of the relation that is revealed (or induced) by co-attendance at events and such expectations can be tested with given

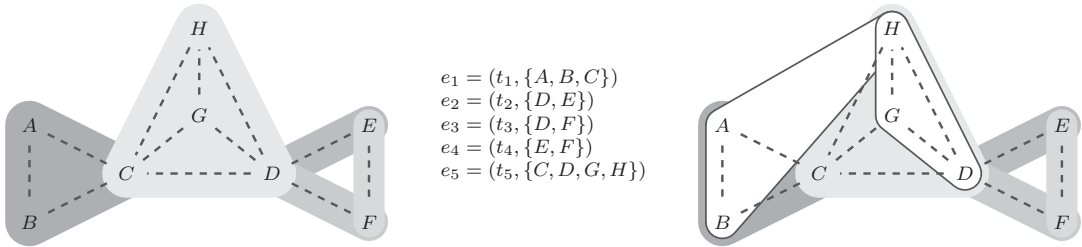


FIG. 4. Illustration of closure on the data from Fig. 1, reproduced from [16]. The hypergraph on the left has been already shown in Fig. 1. Given this history of past events we consider two additional hyperedges $h = \{A, B, H\}$ and $h' = \{D, G, H\}$, on which events could potentially occur, displayed as white areas with dark borders (right). An event on h would point to closure, since actors sharing a common co-participant from previous events (actor C) would get connected for the first time. In contrast, an event on h' could be explained by subset repetition. See the text for additional explanation.

dynamic co-attendance networks. Formally, for a given group of actors $h \subseteq V$, the hyperedge statistic $\text{closure}(t; h; E)$ quantifies to what extent pairs of members of h attended prior events with common third actors $w \in V$ that may be outside of h ; in formulas

$$\text{closure}(t; h; E) = \sum_{\{u, v\} \in \binom{h}{2} \wedge w \neq u, v} \frac{\min[\text{hy.deg}(t; \{u, w\}; E), \text{hy.deg}(t; \{v, w\}; E)]}{\binom{|h|}{2}}.$$

Several variations of the closure effect are possible. For instance, one variation might aggregate the hyperedge degrees $\min[\text{hy.deg}(t; \{u, w, w'\}; E), \text{hy.deg}(t; \{v, w, w'\}; E)]$ for two third actors $w \neq w'$ which are different from the actors $u, v \in h$, or another variation might aggregate the hyperedge degrees $\min[\text{hy.deg}(t; \{u, w\}; E), \text{hy.deg}(t; \{v, w\}; E), \text{hy.deg}(t; \{v', w\}; E)]$ for triples of pairwise different actors $u, v, v' \in h$. Some of these higher-order variants of closure are defined in [21].

We note that considering one-mode projections of co-attendance networks may spuriously suggest a tendency for triadic closure [28]. For instance, a single hyperevent with 10 participants creates 120 closed triangles while not necessarily providing any evidence for triadic closure, since triangles do not necessarily result from closing two paths that were open at the event time. Closure has to be considered jointly with subset repetition of various order [16]. For illustration consider Fig. 4 in which an event on $h = \{A, B, H\}$ would point to closure (actor H is indirectly connected via the third actor C to A and B but has no previous interaction with these two; an event on the hyperedge h therefore closes triangles for the first time). In the same figure, an event on $h' = \{D, G, H\}$ would *not* provide any evidence for closure since all three actors have co-participated in a joint event before so that a hypothetical event on h' could just be explained by partial repetition of participant lists.

In the empirical analysis given in this article we will actually find *negative* closure and argue that this finding—together with positive subset repetition—can explain the emergence of dense, overlapping but stable (i.e. non-merging) groups. As an illustration, see the discussion of Event 5 given in Section 4.6 where we argue that negative closure could explain why this event has the observed participant list, rather than an alternative one that is nearly indistinguishable in all aspects but closure and that would actually cause the two groups to merge.

Computational aspects.

Some definitions of hyperedge statistics given above seem to suggest a high computational runtime. For instance, the definition of subset repetition of order p seems to require to iterate over all subsets of order p of the given hyperedge h —a runtime that would quickly become intractable for even moderately sized p and $|h|$. We note that the implementation of these statistics in the open-source software `eventnet` [16, 56] uses a much more efficient algorithm and is applicable to networks with hundreds of thousands of actors and events; compare [21]. The discussion of these algorithms is out of scope of our current article. Interested readers may learn more about the implementation in the code available from the `eventnet` website.²

3.5 Network descriptives and model evaluation

As discussed above, RHEMs may be specified by including a list of hyperedge statistics in the parametric specification of the event intensity given in Eq. (3.1) and parameters are estimated by maximizing the likelihood given in Eq. (3.2). These maximum likelihood estimates reveal global patterns governing the dynamics of co-attendance networks. To gain concise and generalizable insight, such network effects often assume homogeneity over actors and events. It is assumed that all actors who are similarly embedded in the network of past events display, in expectation, a similar behaviour and it is assumed that all events, in expectation, are governed by the same social rules. Indeed, the contrary assumption—namely that each and every actor potentially behaves differently in each and every event—could only result in a descriptive analysis of co-attendance networks but not in statistically significant and generalizable patterns.

However, we argue that such an unassuming descriptive analysis can effectively *complement*—rather than *replace*—statistical analysis with inferential RHEM. While estimated RHEM parameters may reveal reliable global patterns (i.e. the ‘typical’ behaviour of most actors in most events), tailored qualitative or quantitative descriptive analysis can illuminate deviations from these patterns, such as events that do not fit into the summary explanation offered by RHEM, or individual event participants that occupy uncommon positions in the network of past events.

We propose in the following three methods for descriptive analysis of dynamic co-attendance networks. (1) Dynamic network visualization qualitatively reveals how participants of observed events are embedded in the network of past events. (2) Histograms show how hyperedge statistics (explanatory variables) of each observed event $e = (t_e, h_e)$ are located in the distribution over all alternatives, that is, set of actors $h \subseteq V$ that could have constituted the participant list of the next event—instead of the observed participant list h_e . (3) Histograms showing the distribution of the predicted event rate, computed from the estimated RHEM, reveal how the model-implied probability of each empirically observed event compares to the probabilities over the risk set, that is, the probabilities of alternative set of actors that could potentially have experienced the next event. Figure 5 illustrates these methods on one selected event which is discussed in detail—together with two other representative events—in Section 4.6.

There is a crucial difference between the first two methods (network visualization and distributions of model statistics), and the third one (distribution of the predicted relative event rate). The first two methods are exploratory in the sense that they may be applied *before* RHEM parameters are estimated. Thus, these methods provide descriptions of the empirical *data*—rather than of the model—and might be used qualitatively to assess the validity of homogeneity assumptions, to spot outliers (actors or events with atypical characteristics), or to explore the data in order to gain ideas about which characteristics might

² <https://github.com/juergenlerner/eventnet>

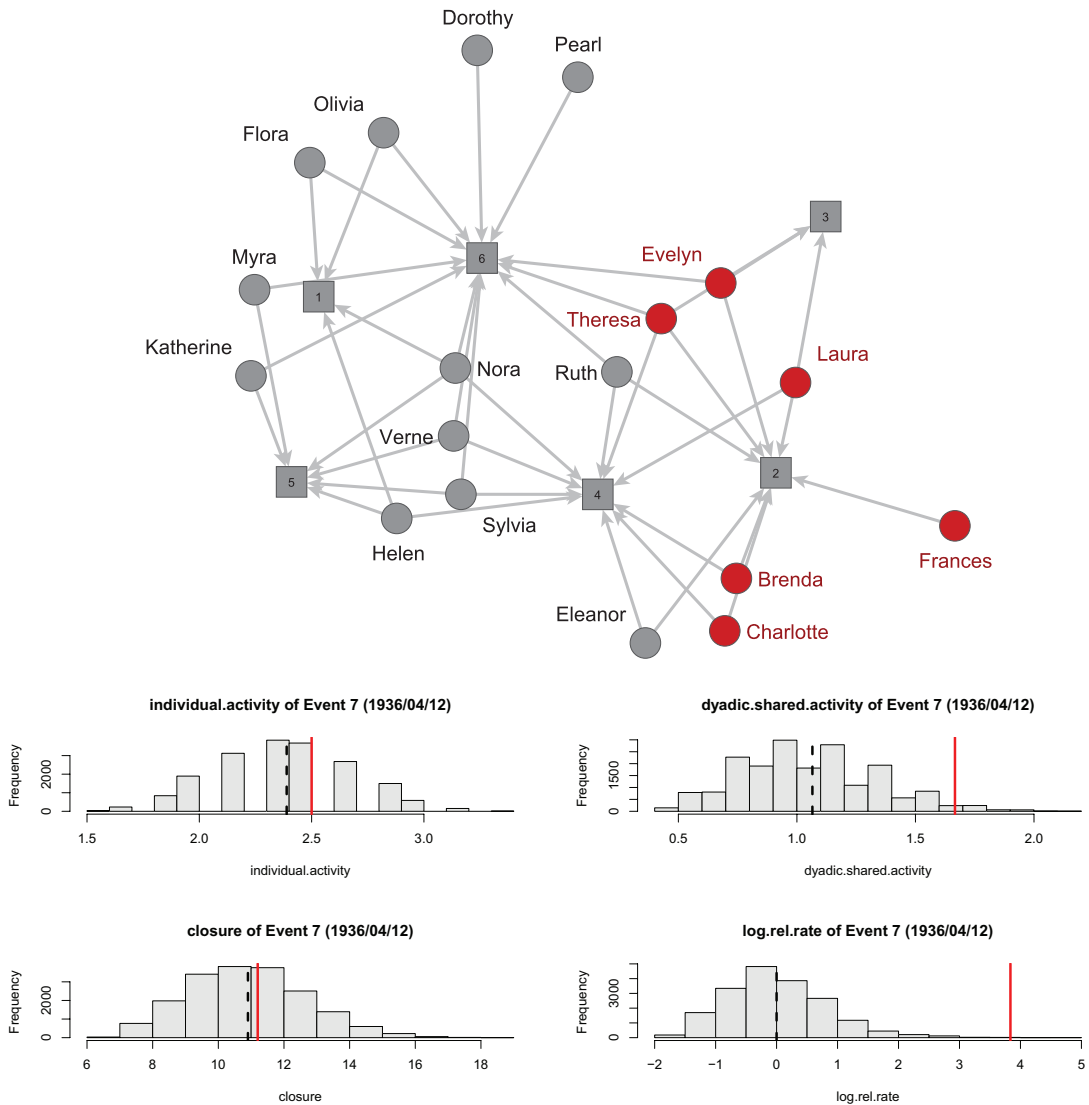


FIG. 5. DGG network shortly before Event 7. The network diagram on top shows how participants of Event 7 (displayed in red) are embedded in the network of the previous six events. The four histograms display the distribution of quantitative statistics over the entire risk set, their mean value (vertical, dashed line), and the value of the single observed Event 7 (vertical, red line). The statistics *individual.activity*, *dyadic.shared.activity* and *closure* are the three statistics used in the specification of the event intensity given in Eq. (3.1). The fourth histogram displays the logarithm of the predicted relative event rate, computed from the RHEM with fitted parameters.

explain co-attendance in events. In contrast, the third method builds upon the RHEM *after* parameters have been estimated and displays how well (or badly) each individual observed event is explained by the model. Thus, the third method is a way to assess model fit and, again, to identify atypical events that do not adhere to the regular patterns followed by the majority of observed events.

3.5.1 Dynamic network visualization For each of the events e_i from the observed sequence of relational hyperevents $E = (e_1, \dots, e_N)$, we visualize the network of past events $G_i = G[E_{<t_{e_i}}]$, showing co-attendance of actors in the events $E_{<t_{e_i}} = e_1, \dots, e_{i-1}$. For each of these networks of past events, we display its two-mode graph as a point-line diagram in which actors are displayed as circles, events are displayed as squares, and actors are connected to the events they have attended by solid lines. The layout (that is the coordinates of the nodes) is computed to simultaneously optimize two criteria. First, distances among nodes in the drawing should best reflect the graph-theoretic distance, that is, the length of shortest paths between nodes. This objective can be achieved by the *stress-minimization* algorithm [73]. The second objective is that node positions in the drawing of G_i should not deviate too much from their positions in the adjacent graphs G_{i-1} and G_{i+1} [74], that is, the dynamic network visualization should have a certain degree of stability allowing to keep a mental map of the network structure. We compute the graph layouts with the visone software [75], which implements the algorithm from [74], simultaneously optimizing both objectives.³

In the visualization of G_i (which shows attendance in the previous events e_1, \dots, e_{i-1}) we highlight the participants of the next event e_i by drawing them in red. See Fig. 5 for the visualization associated with Event 7. The network visualizations of all events are shown in Fig. 6.

3.5.2 Quantitative descriptive statistics Qualitative network visualizations are complemented by quantitative descriptive analysis showing the distributions of hyperedge statistics, that is, of those characteristics that are hypothesized to explain co-attendance at events. Specifically, for each observed event $e = (t_e, h_e)$ we display the statistics of the observed list of participants h_e in relation to the distribution of statistics over all alternatives, that is, hyperedges $h \in R_{t_e}$ in the risk set at the event time. In doing so, we can explore whether observed events typically take particularly high or low (or just average) values in the various statistics and we can spot atypical observed events taking unusual values.

Specifically, let s be a hyperedge statistic, $e = (t_e, h_e) \in E$ be an observed event, and R_{t_e} be the risk set at the event time, that is, the set of alternative hyperedges on which the event at time t_e could potentially have been observed. We display the vector of values $(s(t_e; h; E))_{h \in R_{t_e}}$ in a histogram to show the distribution of the statistic s over the risk set. In this histogram, we additionally display the mean value of s as a dashed, vertical line, and we display the value $(s(t_e; h_e; E))$ that the statistic assumes on the observed set of participants as a vertical red line.

Once the parameters $\hat{\theta}$ of a specific RHEM have been estimated by maximizing the likelihood given in Eq. (3.2), we can compute the model-predicted relative event rate of any hyperedge $h \in R_{t_e}$ by

$$\lambda_1(t_e; h; \hat{\theta}) = \exp\left(\sum_{i=1}^k \hat{\theta}_i s_i(t_e; h)\right),$$

compare Eq. (3.1). We then display the distribution of the logarithm of the predicted relative rate over all hyperedges in the risk set in the same way as we visualize the values of the various statistics.⁴ This approach allows us to assess whether the fitted RHEM does well explain the observed events (by placing

³ The visone software (<https://visone.ethz.ch/>) also allows to produce an animated visualization of the networks at the event times. The animation shows the smooth transition of nodes to their coordinates in the next time step and displays newly created edges in blue. We provide this animation in a dynamic SVG file `DGG_animation.svg` available at <https://github.com/juergenlerner/eventnet/tree/master/data/dgg>.

⁴ We visualize the logarithm of the rate since the raw predicted rates have a very skewed distribution.

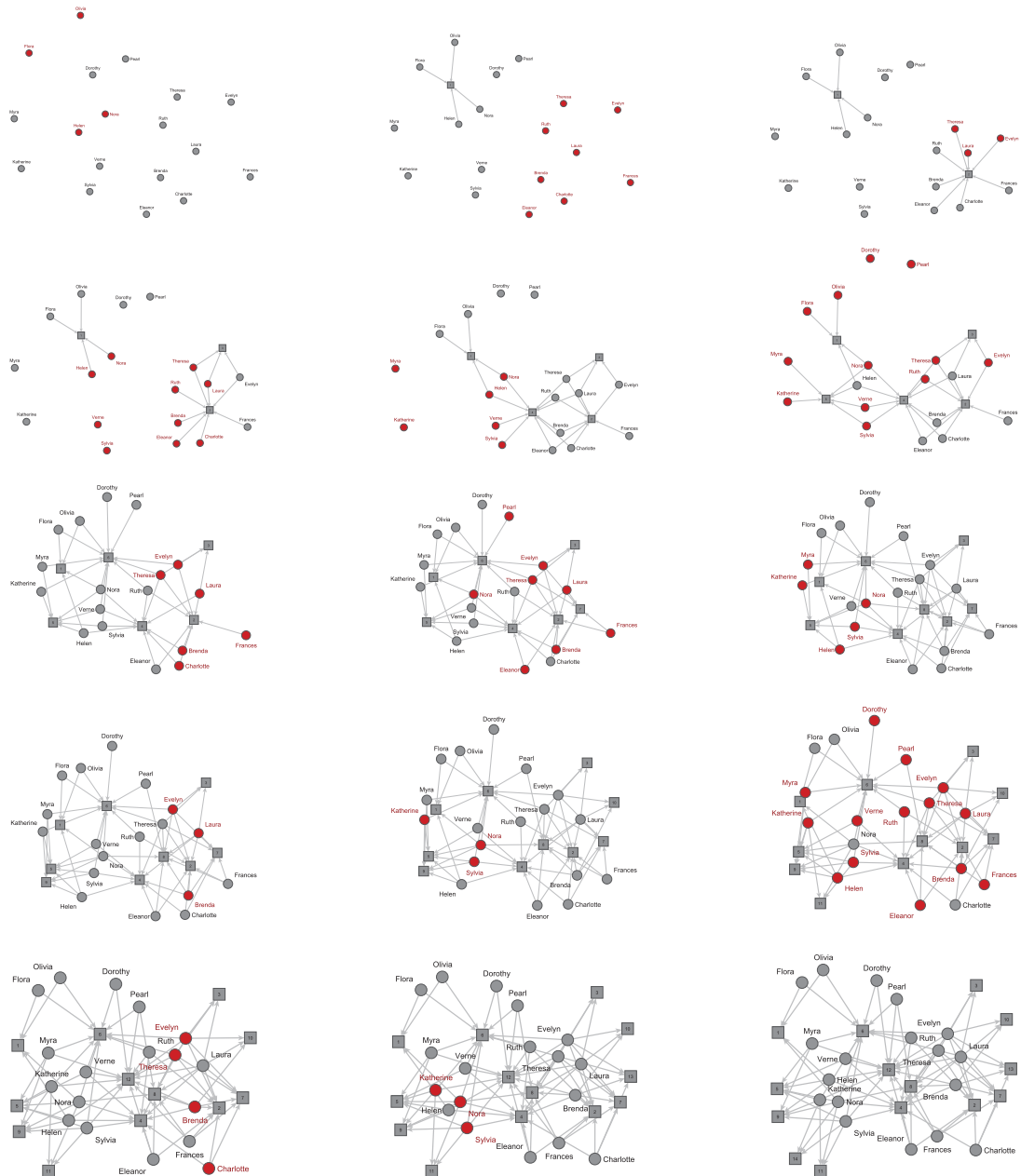


FIG. 6. Network diagrams showing for each event $e_i = e_1, \dots, e_{14}$ in the DGG data how participants of event e_i (displayed in red) are embedded in the network of previous events e_1, \dots, e_{i-1} . The last diagram (in the bottom, right) shows the co-attendance network resulting from all 14 events.

them in the right-hand side of the distribution) and allows to spot atypical observed events that have relatively low rates—according to the model. See Fig. 5 for the histograms associated with Event 7.

3.6 Scope conditions

It is instructive to review the scope conditions necessary for modelling co-attendance networks with RHEM. In general, RHEM are a model for dynamic networks linking actors to the events they attend—but not all types of network dynamics are appropriate for RHEM. In particular we note the following two conditions.

3.6.1 Conditional independence of events. The likelihood function of RHEM given in Eq. (3.2) assumes that the conditional probabilities of events, given the network of past events, are independent. This assumption of conditional independence [76] does not imply that events have to be marginally independent. For instance, an event with a given set of participants h at time t typically increases the probability of observing an event at a later point in time $t' > t$ on a set of participants h' that has a large overlap with h . This kind of dependence could be captured, for example, by the subset repetition effect in RHEM and then does not violate the assumption of *conditional* independence.

In contrast, this assumption is potentially violated if time granularity is low and several events have the same time stamps (i.e. are simultaneous). For the sake of example, let time be given by the week, let t denote a particular week, and let e and e' be two events that could potentially be observed in that week. The assumption of conditional independence would still be valid if it holds that

$$P(e \wedge e' | E_{<t}) = P(e | E_{<t}) \cdot P(e' | E_{<t}),$$

that is, if the conditional probability of observing both events in week t , given the previous events $E_{<t}$ is the product of the conditional probabilities of observing each of these events. In contrast, if it holds that (for instance)

$$P(e \wedge e' | E_{<t}) > P(e | E_{<t}) \cdot P(e' | E_{<t})$$

then the assumption of conditional independence would be violated since the increase in the probability of observing event e' in week t , due to also observing event e , could not be captured by RHEM effects. Note that both events have the same time stamp so that e is not a past event from the point of view of event e' and, thus, e cannot influence the predicted rate of e' in a RHEM.

3.6.2 Simultaneous attendance of actors to events. The second scope condition requires that participants *simultaneously* attend events. If this condition is violated then RHEM—modelling events on sets of actors of any size—are not necessary and the co-attendance network could be analysed by dyadic REM. A well-known example of actor–event networks in which co-attendance is *not* simultaneous is given by boards of directors. Company boards exist over extended periods of time during which individual actors (i.e. directors) can join or leave. Such individual joining or leaving events may depend on current or past composition of boards—and thus it may depend on previous events—but, given that time granularity is sufficiently high so that individual joining and leaving events can be ordered in time, these events are associated with a *dyad* consisting of one director and one company board and can be modelled by dyadic REM [38].

In contrast, events in the DGG data involve more than just two nodes since all event participants simultaneously attend a common event. It would be implausible to model these joint events as a collection of independent dyadic events. In such dynamic co-attendance networks, events are not associated with dyads but rather with hyperedges and, thus, require modelling with relational *hyperevent* models. A similar argument holds for coauthorship networks [11] where scientific papers may be jointly written by any number of authors. A publication event is neither a collection of independent dyadic collaboration events among all pairs of co-authors, nor a collection of independent dyads linking the paper to its authors. Rather than considering a scientific paper as a node in a two-mode network, RHEM consider papers as time-stamped hyperedges connecting the entire set of coauthors in a single hyperevent [21].

4. Empirical illustration: DGG *Southern Women* data

4.1 Reproducibility

RHEM are implemented in the open-source software *eventnet* [16, 56] to hyperevents. Links to the empirical data, software, additional scripts and a step-by-step tutorial for replicating the analysis—along with a description of possible variations—are given in a dedicated page in the *eventnet* wiki.⁵ The small size and famousness of the DGG data makes it ideal for illustrating the practical use of RHEM.

4.2 Testing the model on a canonical dataset

We illustrate the empirical use of RHEM—along with the descriptive analysis of dynamic co-attendance networks—on the well-known *Southern Women* data collected by [26], which records co-attendance of 18 actors (women) at 14 social events in ‘Old City’, (actually Natchez, Mississippi) reproduced in Table 1. Examples of events attended by the ‘Southern Women’ include a church supper and a card party. Note that—since our focus is on the temporal evolution of this network—we have chosen to number events in chronological order (for comparison, the event codes assigned by [26] are also given in the table). The DGG network is one of the most frequently used datasets in the network analysis of social groups [27]. Despite the fact that event times are reported in the original publication, surprisingly few papers actually exploit these event times or their chronological ordering, with notable exceptions including [9, 77].

The time independent macro structure of this network is a decomposition into two dense subgroups or clusters which—according to the meta-analysis of [27]—are given by the two sets

$$\{Evelyn, Laura, Theresa, Brenda, Charlotte, Frances, Eleanor, Pearl, Ruth\}$$

$$\{Verne, Myra, Katherine, Sylvia, Nora, Helen, Dorothy, Olivia, Flora\}.$$

The meta-analysis of [27] also makes it clear that at least some membership in these dense subgroups is debatable because the women have varying degree of membership into one or both of the two subgroups, and occupy different positions in a core–periphery scale. For example, in an earlier reanalysis, [78] identified *Pearl, Ruth, Verne, Dorothy, Olivia, Flora* as not belonging clearly to either subgroup. We note that our network visualizations qualitatively confirm the clusters given above (see e.g. Fig. 7) and our descriptive analysis reveals that the majority of events are clearly located within one of the two clusters.

⁵ [https://github.com/juergenlerner/eventnet/wiki/RHEM-first-steps-\(tutorial\).](https://github.com/juergenlerner/eventnet/wiki/RHEM-first-steps-(tutorial).)

TABLE 1 DGG co-attendance network, reproduced from Fig. 3 of Ref. [26]. Note that in this table, events are ordered from left to right in chronological order: DGG code is the event code that has been chosen by [26] in an order that reveals the clustering of the actor–event network. Dates of events are in the format month/day and are all in the year 1936

Event id	1	2	3	4	5	6	7	8	9	10	11	12	13	14
DGG code	11	5	2	7	12	9	3	6	10	1	14	8	4	13
Date	2/23	2/25	3/2	3/15	4/7	4/8	4/12	5/19	6/10	6/27	8/3	9/16	9/26	11/21
Nora	×	.	.	×	×	×	.	×	×	.	×	.	.	×
Helen	×	.	.	×	×	.	.	·	×	.	·	×	.	.
Olivia	×	.	.	.	·	×	.	·	·	·	·	·	·	.
Flora	×	.	.	.	·	×	.	·	·	·	·	·	·	.
Evelyn	.	×	×	·	·	×	×	·	·	×	·	·	×	.
Laura	.	×	×	×	·	·	×	·	·	×	·	·	·	.
Theresa	.	×	×	×	·	·	×	·	·	·	·	·	·	.
Brenda	.	×	·	×	·	·	·	·	·	·	·	·	·	.
Charlotte	.	×	·	·	·	·	·	·	·	·	·	·	·	.
Frances	.	×	·	·	·	·	·	·	·	·	·	·	·	.
Eleanor	.	×	·	·	·	·	·	·	·	·	·	·	·	.
Ruth	.	×	·	·	·	·	·	·	·	·	·	·	·	.
Verne	.	.	·	·	·	·	·	·	·	·	·	·	·	.
Sylvia	.	.	·	·	·	·	·	·	·	·	·	·	·	·
Myra	.	.	·	·	·	·	·	·	·	·	·	·	·	.
Katherine	.	.	·	·	·	·	·	·	·	·	·	·	·	·
Pearl	.	.	·	·	·	·	·	·	·	·	·	·	·	.
Dorothy	.	.	·	·	·	·	·	·	·	·	·	·	·	.

Our method does not rely on any crisp partitioning into subgroups—and, in fact, it does not compute any explicit subgroups. However, for every subset of actors (i.e. for every hyperedge) and for every point in time, we can compute the values of hyperedge statistics, such as subset repetition, indicating the frequency of previous joint events among members of the subset—thereby giving a strength of association by prior joint participation among the members of the given subset.

While a network given by 14 observations (events) involving in total 18 actors seems to be rather small for analysis with inferential network models, we argue that it is exactly the manageability of the data size—along with its widespread popularity—that makes the DGG data a perfect use case for *illustrating RHEM*. The small network size allows us to augment statistically significant results, obtained by fitting RHEM to the data, with quantitative descriptive statistics of each event and with qualitative network visualizations showing the positions of event participants in the evolving co-attendance network. The combination of these methods provides a unique connection from the observed data—and the characteristics of events and their constituting participants—to the final conclusions supported by empirically estimated RHEMs. By doing so we provide a proof of concept that RHEM do not only apply to large networks (see e.g. the second case study given in [21]) but also have the potential to ‘scale down’ to individual cases [29]. Since the DGG data comprises only 14 observations, we cannot fit models specified with a large number

of RHEM statistics—nor can we include RHEM terms of very high complexity (e.g. subset repetition of high order). We refer readers interested in RHEM estimated on larger datasets to, for example, [16, 21] or to other case studies reported in the tutorials for the *eventnet* software.

4.3 Orienting questions

We organize our illustrative analysis around three orienting research questions explaining joint participation in events which—in the absence of endogenously given actor-level covariates—are three of the most common effects specified in studies of event networks. We emphasize that in this article we do not develop any hypotheses concerning these effects, but rather we consider the analysis as exploratory.

RQ1 **(individual activity)** Does the propensity of a group to jointly attend events increase with the number of prior events individually attended by its members.

RQ2 **(shared activity/familiarity)** Does the propensity of a group to jointly attend events increase with the number of prior shared events co-attended by pairs or triples of its members.

RQ3 **(closure)** Does the propensity of a group to jointly attend events increase with the number of prior shared events co-attended by its members with common third actors.

Together, the questions that orient the empirical analysis are important for empirical studies interested in predicting patterns of participation to future events given participation in past events, and understanding the mechanisms out of which social structure emerges from individual attention allocation decisions. These research questions are particularly appropriate for the purpose of illustrating the empirical value of RHEM since they refer to near-universal mechanisms shaping the structure of networks of multi-actor events, almost regardless of the specific empirical setting. Whether or not a given empirical study is concerned with these questions, the corresponding effects should at least be included to control for baseline effects in relational hyperevent networks.

4.4 Empirical model specification

We fit RHEM specified by (combinations of) four hyperedge statistics matching the given orienting questions: subset repetition of order one ('individual activity'), two ('dyadic shared activity') and three ('triadic shared activity') and triadic closure. Subset repetition of order one addresses RQ1 about the effect of prior individual activity: are actors who—individually—attended more events in the past also more active attendees in the future. Subset repetition of order two (one of the two effects related with RQ2) assesses the effect of dyadic familiarity: does the propensity to co-attend events increase with the number of prior dyadwise shared events? Subset repetition of order three (the other effect related with RQ2) assesses whether triadic familiarity has an additional effect over prior dyadwise shared events. Addressing RQ3, closure assesses whether groups of actors that have prior events with common third actors (potentially outside of the group) have an increased propensity to experience a joint event themselves. We fit three models: Model 1 includes individual activity and closure, Model 2 additionally includes dyadic shared activity, and Model 3 additionally includes triadic shared activity.

Once the hyperedge statistics have been computed for all elements in the risk sets (observed events and non-event hyperedges), RHEM parameters can be estimated with standard statistical software for

TABLE 2 *RHEM estimates from the DGG data. All models have been fitted with 14 observed events and 207,964 non-event hyperedges—the union of the size-constrained risk sets at the event times.*

	Model 1	Model 2	Model 3
individual.activity	−0.44 (0.83)	−3.71 (1.19)**	−4.11 (1.76)*
dyadic.shared.activity		7.32 (1.70)***	8.33 (3.67)*
triadic.shared.activity			−0.68 (2.17)
closure	0.41 (0.17)*	−0.52 (0.26)*	−0.52 (0.26)*
AIC	234.83	208.55	210.45

*** $p < 0.001$, ** $p < 0.01$, * $p < 0.05$.

survival analysis. To estimate the RHEM parameters reported below, we compute hyperedge statistics with `eventnet`⁶ [16, 56] and use the R package `survival`⁷ [66] to estimate parameters.

4.5 Results

Table 2 reports RHEM parameter estimates from the DGG data. In that table, we write *individual activity* for subset repetition of order one, *dyadic shared activity* for subset repetition of order two, and *triadic shared activity* for subset repetition of order three.

When comparing the model fit indicator AIC (recall that lower values indicate better fit), we find that Model 2, comprising the effects prior individual activity, prior dyadwise shared activity, and closure has the best fit. Adding prior dyadwise shared activity to Model 1 implies a large improvement in the model fit; additionally including triadic shared activity slightly decreases model fit.

Turning to the sign and significance of the individual effects, we find that prior dyadwise shared activity is consistently and significantly positive. Thus, groups of actors are more likely to attend joint events if members of these groups have pairwise jointly attended past events. This effect is likely to reinforce dense groups of actors co-attending the same events. Triadic shared activity is not statistically significant when controlling for dyadic familiarity. This could result from the rather small data size whose 14 observed events seem to be insufficient to separate the effects of too many closely related statistics.

Closure is significantly negative in Models 2 and 3—but is significantly positive in Model 1 which fails to control for prior shared activity. The negative closure effect reveals that overlapping dense groups have a reluctance to merge over time. Thus, brokers have a tendency to maintain their brokerage roles. The positive closure effect in Model 1—which fails to control for shared activity—is likely to be a spurious effect. This happens since events are often partially repeated within dense groups which implies higher than average closure statistic. However, after controlling for prior shared activity, closure becomes consistently negative.

The parameter associated with prior individual activity is significantly negative in all models that also include dyadic shared activity (and not significant in Model 1). Prior individual activity and prior shared activity have to be understood in combination. Assume, for the sake of example, that there are two groups $\{A_1, A_2, A_3\}$ and $\{B_1, B_2, B_3\}$ each consisting of three actors and first assume that each of these

⁶ <https://github.com/juergenlerner/eventnet>

⁷ <https://CRAN.R-project.org/package=survival>

groups co-attended one common three-actor event. Since dyadic shared activity has a significantly and strong positive effect it follows that dyads within groups, such as $\{A_1, A_2\}$ or $\{B_1, B_2\}$, have an increased probability to co-participate in a future event. In contrast, dyads consisting of actors from different groups, such as $\{A_1, B_1\}$ or $\{A_1, B_2\}$, have no prior shared event and, by the negative effect of individual activity, have a decreased probability to co-participate in a future event. Thus, intuitively, actors have a preference to co-participate with those of their in-group but an aversion to co-participate in events with actors from the out-group. Now assume that each of the two groups attended two (instead of one) common three-actor event in the past. By the positive effect of dyadic shared activity, the likelihood of further events within the groups would increase—but, by the negative effect of individual activity, the likelihood of events mixing members from the two groups would decrease. Thus, the additional joint events increase the actors' perception of who is in their in-group (attractive choices for co-participation in future events)—but they also increase the actors' perception of who is in the out-group (unattractive choices for co-participation in future events). The negative parameter associated with individual activity, therefore, does not imply that actors who were more active in the past are less active in the future—it just implies that they are less likely to co-participate in events with those with which they do not share prior common events, that is, with unfamiliar actors.

We additionally fitted a model specified with individual activity and dyadic shared activity but excluding the closure statistic (not reported in this article). We found no qualitative change in parameter signs or significance levels. That model without the closure effect has a weaker model fit (i.e., higher AIC) than Model 2 in Table 2.

In summary, the DGG network is characterized by a tendency to reinforce dense groups (positive effect of shared activity) and a tendency *not* to merge overlapping dense groups (negative effect of closure), where the latter effect points to the maintenance of stable broker positions.

4.6 Zooming in on specific events

We now enrich the understanding of RHEMs by discussing how the group of participants in three selected events are located in the space of all alternatives (i.e. groups of actors that could have constituted the participant lists at the event times). We connect the statistically significant network effects revealed by model estimation to the data that were actually observed. We concentrate on the best-fitting Model 2 from Table 2 and consider the position of the group of event participants from two angles: (1) descriptive statistical graphics highlight how quantifiable characteristics (i.e. model statistics) of the event's participant list compare to the respective characteristics of alternative groups from the risk set and (2) appropriate network visualizations show how the group of participants of the respective event are located in the network of past events. Our objective in this post-estimation analysis is to test the ability of the model to support qualitative insight at the level of individual events.

For three specific events—namely Event 7, Event 4 and Event 5—we display the network of past events at the event times, as well as the distributions of statistics, in Figs 5, 8 and 9. We choose to discuss precisely these three events since they represent distinct *types* of events. Event 7 is one with the highest relative event rate, according to the model, and is broadly representative for about half of the 14 observed events, mostly connecting participants from only one of the two clusters. Event 4 is the one with the lowest relative event rate in the observed sequence of events—it connects actors from both clusters—and is one of only two of the 14 observed events that are deemed by the model to be less likely than the average over their alternatives. Event 5 has a relative event rate that is also considerably higher than average—but it does so in a very unusual way since it takes rather low values in all three model statistics (in contrast,

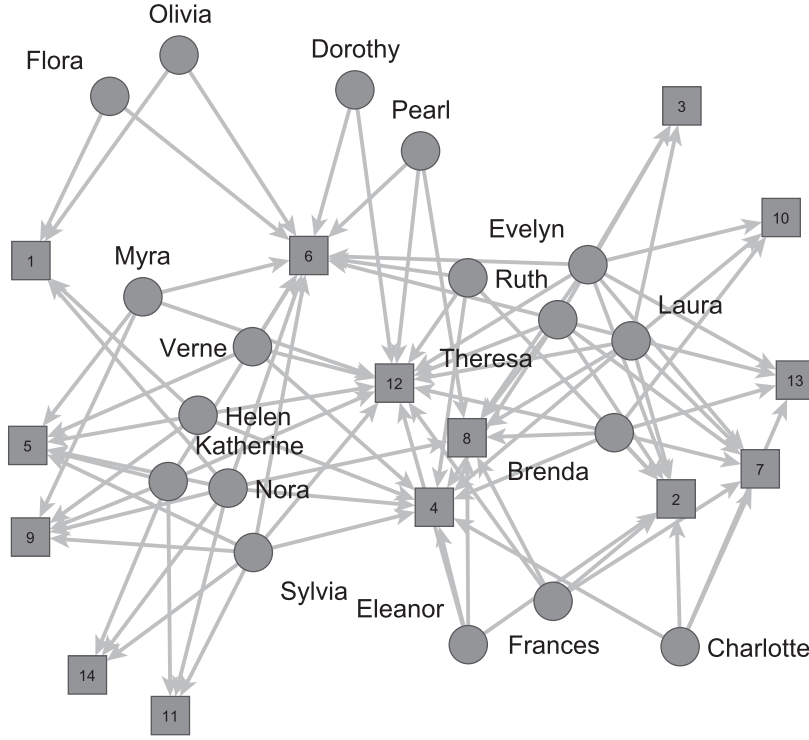


FIG. 7. DGG network after the last event (Event 14).

most observed events take above-average values in all three model statistics). We note that the network visualizations and statistical graphics of all 14 events can be found in the Supporting Information.

4.6.1 Event 7 (12 April 1936). The network visualization and distributions of statistics of Event 7 are shown in Fig. 5. The network visualization at the time of Event 7 displays all previous events, that is, Event 1 to Event 6. Additionally, the participants of Event 7 are highlighted in red.

Event 7 has as participant list (i.e. hyperedge) the set

$$h_7 = \{Evelyn, Laura, Theresa, Brenda, Charlotte, Frances\}.$$

These actors are mostly members of one of the two evolving cluster, centred around the past Event 2, and Event 7 actually involves a proper subset of the participants of Event 2. Due to this history, the event hyperedge h_7 has a prior dyadwise shared activity that is far above the average and in the right tail of the distribution of all alternative hyperedges at the event time (which are all sets of exactly six actors). On the other hand, prior individual activity and closure (which both have a negative effect on the event rate) are only slightly above average.

Quantitatively, we have $dyadic.shared.activity(t_7, h_7) = 1.67$ which is 0.6 more than the average (mean) value over the risk set: $mean\{dyadic.shared.activity(t_7, h) ; h \in R_{t_7}\} = 1.07$. By the associated

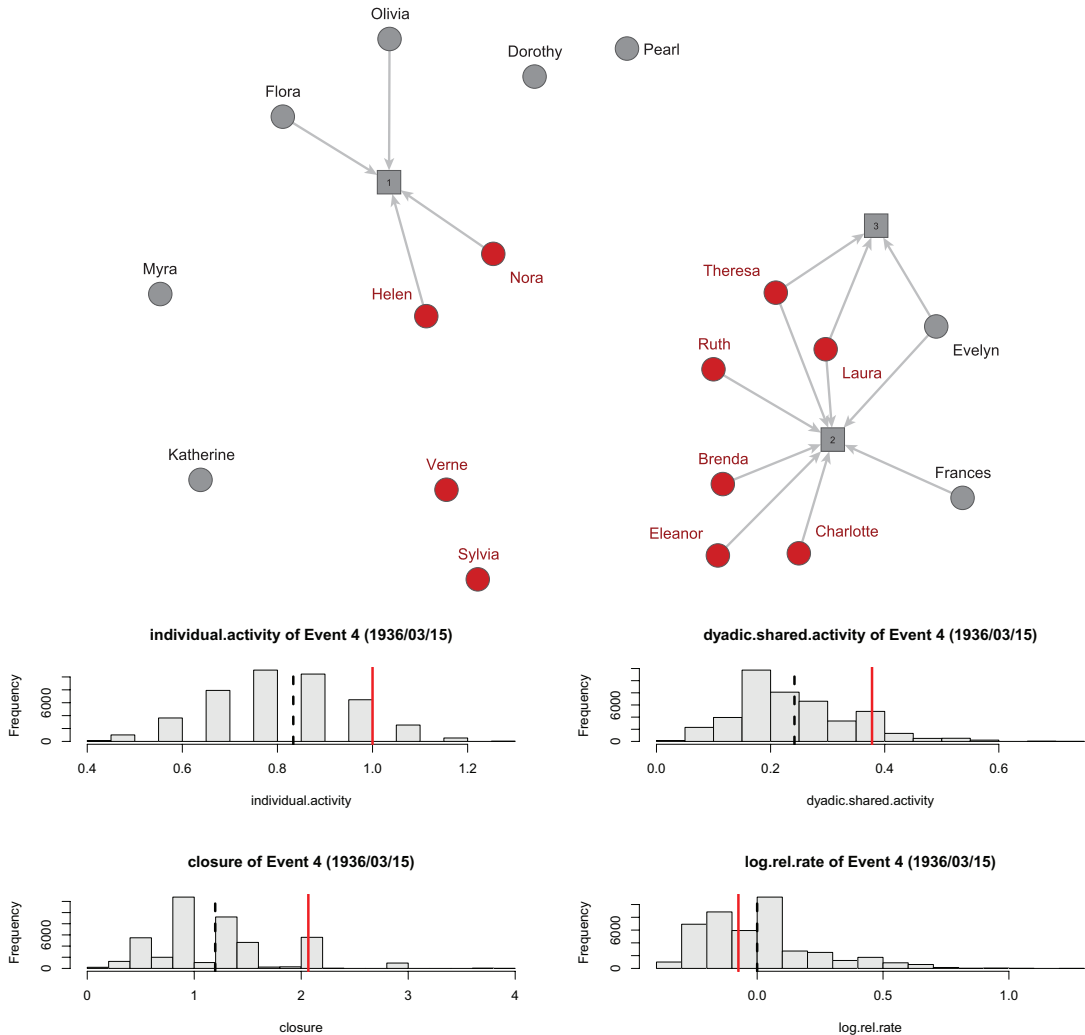


FIG. 8. DGG network shortly before Event 4 whose participants are displayed in red. Event 4 is the most unlikely in the whole sequence (according to the model). It bridges between the two emerging groups.

model parameter (equal to 7.32), the higher value in the dyadic shared activity alone implies a predicted event rate for h_7 that is equal to $\exp(7.32 \cdot 0.60) = 81.65$ times the average rate over the risk set. This increase, however, is offset in part by the negative effects of prior individual activity and closure. We have that the prior individual activity of h_7 (equal to 2.5) is by 0.11 higher than the average value over the risk set (equal to 2.39). This implies a multiplication of the event rate—explained by the higher value of individual activity—by $\exp(-3.71 \cdot 0.11) = 0.66$ (thus, the estimated rate is decreased by 34%). Moreover, we have that closure on h_7 is 11.2 and thus by 0.30 higher than the average (10.90), implying a multiplication of the event rate of $\exp(-0.52 \cdot 0.30) = 0.86$ —a decrease of 14%.

Taking the three model effects together, we obtain that the predicted event rate on hyperedge h_7 at time t_7 is—according to the model—higher than average by a factor of $\exp(-3.71 \cdot 0.11 + 7.32 \cdot 0.60 - 0.52 \cdot 0.30) = 46.32$. Indeed, the histogram for the logarithm of the relative event rate shows that the rate of h_7 is far in the right tail. More precisely, among the $\binom{18}{6} = 18,564$ hyperedges in the size-constrained risk set associated with Event 7, only nine hyperedges have a predicted event rate that is higher than that of h_7 . Event 7 is broadly representative for several of the most likely events, namely Events 3, 7, 9, 10, 11, 13 and 14, which involve mostly actors from only one of the two emerging groups. It is striking that most of these within-group events take place in the second half of the event sequence—suggesting that group formation takes time and actors’ perception of who is in their in-group or out-group gets stronger over time, pointing to a reinforcement effect of perceived group membership.

4.6.2 Event 4 (15 March 1936). The network visualization and distributions of statistics of Event 4 are shown in Fig. 8. Event 4 is the one with the lowest relative probability in the sequence of observed events—according to the model. Event 4 involves the 10 participants

$$h_4 = \{Laura, Theresa, Brenda, Charlotte, Eleanor, Ruth, Verne, Sylvia, Nora, Helen\}.$$

Event 4 can be described as an event that connects previously disparate sets of actors. While all three model statistics are above average, the value of the dyadic shared activity is too low to offset the negative effect of individual activity and closure. More precisely, the effect of dyadic shared activity multiplies the predicted event rate on h_4 by a factor of 2.71. On the other hand, the effect of individual activity decreases the estimated event rate by a factor of 0.54 and closure decreases the predicted event rate on h_4 by a factor of 0.64. Taking the three effects together, an event on h_4 at time t_4 is predicted to have an event rate that is 0.93 times the average rate—a decrease of 7%. There are only two events in the given sequence of 14 events that have a below-average predicted event rate, according to the model. These ‘unlikely’ events are Event 4 and Event 12, where the predicted rate of Event 12 is only slightly below average.

4.6.3 Event 5 (7 April 1936). The network visualization and distributions of statistics of Event 5 are shown in Fig. 9. Event 5 is an interesting event: it has values *below* average in all three model statistics—in stark contrast to the majority of observed events—but its predicted event rate is nevertheless higher than average, according to the model. Event 5 involves the six actors

$$h_5 = \{Verne, Myra, Katherine, Sylvia, Nora, Helen\}.$$

From the visualization we could judge that Event 5 connects formerly disparate sets of actors—and indeed its prior dyadwise shared activity is below average, decreasing the predicted event rate. However, while dyadic shared activity is only slightly below average, both individual activity and closure are by a larger margin below average—increasing the predicted event rate. Thus, an event on h_5 has a higher than average rate (by a factor of 3.84) because, for an event with such low values in individual activity and closure, it has relatively high prior shared activity.

It is informative to compare the hyperedge h_5 , on which the Event 5 has been observed, with the alternative hyperedge

$$h = \{Flora, Olivia, Theresa, Ruth, Laura, Brenda\},$$

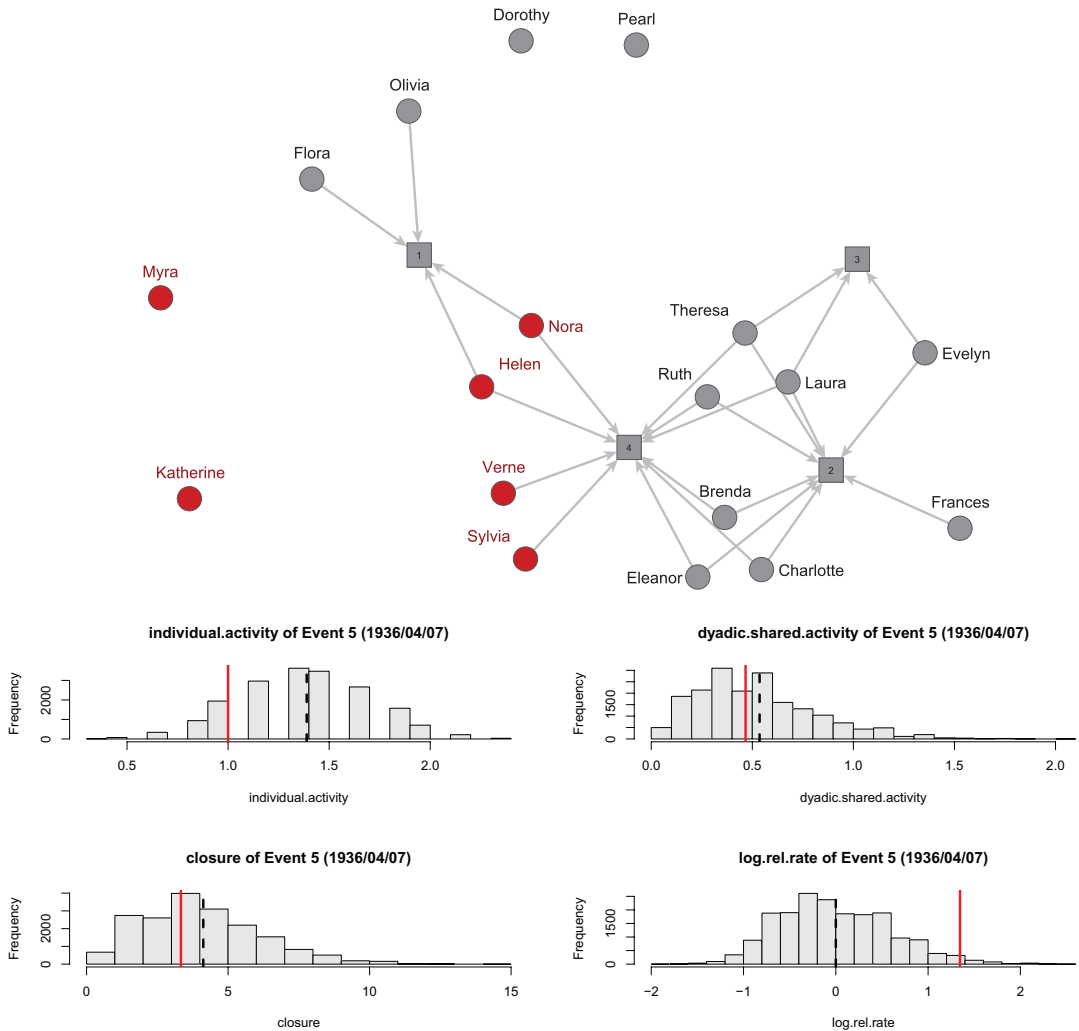


FIG. 9. DGG network shortly before Event 5 whose participants are displayed in red. Event 5 has below-average values in all three statistics—its probability is nevertheless above average, according to the model.

which has the same size as h_5 and is therefore a member of the risk set R_{h_5} . An event on this alternative hyperedge would close many open two paths—namely those connecting Flora and Olivia on one hand, over the bridging actors Nora and Helen, with the dense cluster Theresa, Ruth, Laura and Brenda. The alternative hyperedge h has—compared to the actually observed event hyperedge h_5 —higher values in individual activity (plus 1.0), in dyadic shared activity (plus 0.47), but most remarkably in closure (plus 3.53). According to the model, the rate-decreasing effect of the higher individual activity approximately cancels out the rate-increasing effect of the higher shared activity. What remains is the rate-decreasing effect of the higher value of closure. Indeed, considering all three effects, the model predicts an event rate on the alternative hyperedge h that is only 0.12 (i.e. 12%) of the predicted rate on the observed

hyperedge h_5 . This illustrates that the negative closure effect is important to prevent events on hyperedges like h which would close structural holes and would cause the two dense groups to merge.

Overall we find that most observed events are rather well explained by Model 2 from Table 2. In fact, just two out of 14 observed events have a predicted event rate that is lower than the average over alternative participant lists. Most events are assigned high relative event rates by the model since they are clearly located within one of the two emerging clusters. Yet, a small number of events (e.g. Event 5) have low values in the prior shared event statistic—and thus, connect previously weakly connected actors. However, these ‘bridging events’ can still be assigned a higher than average event rate by the model, if they are composed of formerly rather inactive actors, and/or are characterized by low values in the closure statistic.

5. Discussion and conclusion

Almost by definition ‘events’ occupy a unique position in time. This simple observation suggests a representation of events as hyperedges connecting multiple actors simultaneously attending non-repeatable, time-specific events. A time-ordered sequence of events gives rise to an evolving hypergraph with emergent structural properties induced by patterns of individual participation. Relational hyperevent models (RHEMs) may be adopted to study the dynamics of mutual constitution of individuals and events they attend (or ‘groups’ in which they participate). The model makes full use of the multilevel structure of hyperevent networks simultaneously affiliating multiple lower level units (individuals in the case we have discussed) to multiple higher level units (events in our case).

RHEMs can be specified to test hypotheses about social mechanisms affiliating individuals to events. But RHEMs can also be specified to study where observed events are located in the space of possible events that could have taken place—but did not. This last feature, in particular, illustrates the new analytical possibilities offered by a model that may be scaled up at the level of millions of nodes [16, 56], and just as easily scaled down to examine individual ‘cases’ thus illustrating the ‘duality of scaling up and down’ [29, p. 3].

The possibility of specifying the multiple processes of mutual constitution linking ‘agentic’ and ‘structural’ levels of action [79] is what makes RHEMs unique as models for characterizing the duality of individuals and groups. The illustrative analysis that we have presented provides a clear demonstration of this claim. The goal of the original study by DGG was to identify the clique structure—the social cleavages—among the Southern Women in ‘Old City’. Multiple secondary analyses of the same data [27] have confirmed the presence of partially overlapping subgroups—although there is no clear consensus about the number of groups and their precise composition. While the objective of the model we have presented was not to identify the number of social groups, we note that the negative coefficient associated with the triadic closure effect indicates a clear tendency of the affiliation of women to events to sustain a differentiated pattern of participation. The tendency against closure suggests that dense and partially overlapping groups may be reluctant to merge and tend to remain separate over time. Individual participation in events produces—but at the same time is a product of this structural tendency. Further analysis reveals that events that may potentially close multiple open 2-paths existing among participants across events are unlikely to happen.

Clearly, the empirical case we have presented does not provide a final demonstration of the general usefulness or applicability of RHEMs. The data we have analysed have all the advantages of data that are generally recognized as canonical [27], and all the disadvantages of secondary data that preclude access to the original sources and social setting—as noted also by [3] in his re-analysis of the ‘Southern Women’ data. Yet, our view is that the theoretical scope, empirical applicability, and computational

flexibility of RHEMs easily transcend the relatively narrow boundaries of the illustrative analysis that we have offered in this article. The theoretical scope of RHEMs is broad because the mechanisms of mutual constitution across levels of action that we specified are not dependent on any particular social setting, or situation. The empirical applicability of RHEMs is similarly broad because multicast interaction is a common feature of social relations be they face-to-face like, for example, conversation [62], or mediated by technology like, for example, e-mail [24]. Computationally, RHEMs are member in a class of flexible REMs whose reliability and efficiency have been extensively tested [56]. The scaling properties of this class of models make them particularly useful for the analysis of very large networks. This article demonstrates a comparable value of RHEMs for the analysis of small networks of social events.

Funding

The Deutsche Forschungsgemeinschaft (DFG) (321869138).

REFERENCES

1. MÜTZEL, S. & BREIGER, R. (2020) Duality beyond persons and groups. *The Oxford Handbook of Social Networks* (R. Light & J. Moody eds). Oxford University Press, pp. 392.
2. BREIGER, R. L. (2002) Poststructuralism in organizational studies. *Social Structure and Organizations Revisited* (M. Lounsbury & M. Ventresca, eds). Emerald Group Publishing Limited, pp. 295–305.
3. BREIGER, R. L. (1974) The duality of persons and groups. *Soc. Forces*, **53**, 181–190.
4. BREIGER, R. L. (2000) A tool kit for practice theory. *Poetics*, **27**, 91–115.
5. BREIGER, R. L. (2009) On the duality of cases and variables: correspondence analysis (CA) and qualitative comparative analysis (QCA). *The SAGE Handbook of Case-based Methods* (D. Byrne & C. C. Ragin eds). SAGE, pp. 243–259.
6. BREIGER, R. L. & MOHR, J. W. (2004) Institutional logics from the aggregation of organizational networks: operational procedures for the analysis of counted data. *Comput. Math. Organ. Theory*, **10**, 17–43.
7. MELAMED, D., BREIGER, R. L. & SCHOON, E. (2013) The duality of clusters and statistical interactions. *Sociol. Methods Res.*, **42**, 41–59.
8. PACHUCKI, M. A. & BREIGER, R. L. (2010) Cultural holes: beyond relationality in social networks and culture. *Annu. Rev. Sociol.*, **36**, 205–224.
9. EVERETT, M. G., BROCCATELLI, C., BORGATTI, S. P. & KOSKINEN, J. (2018) Measuring knowledge and experience in two mode temporal networks. *Soc. Netw.*, **55**, 63–73.
10. KREBS, V. (2002) Uncloaking terrorist networks. *First Monday*.
11. NEWMAN, M. E. (2004) Coauthorship networks and patterns of scientific collaboration. *Proc. Natl. Acad. Sci. USA*, **101**(suppl 1), 5200–5205.
12. SORENSEN, O. & STUART, T. E. (2008) Bringing the context back in: settings and the search for syndicate partners in venture capital investment networks. *Admin. Sci. Q.*, **53**, 266–294.
13. BATAGELJ, V., FERLIGOJ, A. & SQUAZZONI, F. (2017) The emergence of a field: a network analysis of research on peer review. *Scientometrics*, **113**, 503–532.
14. CONALDI, G. & LOMI, A. (2013) The dual network structure of organizational problem solving: a case study on open source software development. *Soc. Netw.*, **35**, 237–250.
15. LERNER, J. & LOMI, A. (2020a) The free encyclopedia that anyone can dispute: an analysis of the micro-structural dynamics of positive and negative relations in the production of contentious Wikipedia articles. *Soc. Netw.*, **60**, 11–25.
16. LERNER, J., LOMI, A., MOWBRAY, J., ROLLINGS, N. & TRANMER, M. (2021) Dynamic network analysis of contact diaries. *Soc. Netw.*, **66**, 224–236.

17. BRANDES, U., LERNER, J. & SNIJDERS, T. A. (2009) Networks evolving step by step: statistical analysis of dyadic event data. *Proceedings of International Conference on Advances in Social Network Analysis and Mining (ASONAM)* (N. Memon & R. Alhajj eds). IEEE Computer Society, pp. 200–205.
18. BUTTS, C. T. (2008) A relational event framework for social action. *Sociol. Methodol.*, **38**, 155–200.
19. BERGE, C. (1989) *Hypergraphs: Combinatorics of Finite Sets*. North-Holland.
20. WASSERMAN, S., FAUST, K. ET AL. (1994) *Social Network Analysis: Methods and Applications*. Cambridge University Press.
21. LERNER, J., TRANMER, M., MOWBRAY, J. & HANCEAN, M.-G. (2019) REM beyond dyads: relational hyperevent models for multi-actor interaction networks. *arXiv preprint arXiv:1912.07403*. <https://arxiv.org/abs/1912.07403>.
22. HÂNCEAN, M.-G., LERNER, J., PERC, M., GHÎȚĂ, M. C., BUNACIU, D.-A., STOICA, A. A. & MIHĂILĂ, B.-E. (2021) The role of age in the spreading of COVID-19 across a social network in Bucharest. *J. Complex Netw.*, **9**.
23. STADTFELD, C. & BLOCK, P. (2017) Interactions, actors, and time: dynamic network actor models for relational events. *Sociol. Sci.*, **4**, 318–352.
24. PERRY, P. O. & WOLFE, P. J. (2013) Point process modelling for directed interaction networks. *J. R. Stat. Soc.*, **82**, 821–849.
25. VU, D., LOMI, A., MASCIA, D. & PALLOTTI, F. (2017) Relational event models for longitudinal network data with an application to interhospital patient transfers. *Stat. Med.*, **36**, 2265–2287.
26. DAVIS, A., GARDNER, B. & GARDNER, M. (1941) *Deep South*. The University of Chicago Press.
27. FREEMAN, L. C. (2003) Finding social groups: a meta-analysis of the Southern Women data. *Dynamic Social Network Modeling and Analysis: Workshop Summary and Papers* (R. Breiger, C. Carley, & P. Pattison eds). Washington, DC: National Research Council, The National Academies Press, pp. 39–97.
28. BORGATTI, S. P. & EVERETT, M. G. (1997) Network analysis of 2-mode data. *Soc. Netw.*, **19**, 243–270.
29. BREIGER, R. L. (2015) Scaling down. *Big Data & Soc.*, **2**, 2053951715602497.
30. MOHR, J. W. & DUQUENNE, V. (1997) The duality of culture and practice: poverty relief in New York City, 1888–1917. *Theory Soc.*, **26**, 305–356.
31. MISCHE, A. & PATTISON, P. (2000) Composing a civic arena: publics, projects, and social settings. *Poetics*, **27**, 163–194.
32. PINCH, T. & TROCCO, F. (1998) The social construction of the early electronic music synthesizer. *Icon*, 9–31.
33. MISCHE, A. & WHITE, H. (1998) Between conversation and situation: public switching dynamics across network domains. *Soc. Res.*, 695–724.
34. AMATI, V., LOMI, A., MASCIA, D. & PALLOTTI, F. (2021) The co-evolution of organizational and network structure: the role of multilevel mixing and closure mechanisms. *Organ. Res. Methods*, **24**, 285–318.
35. KOVÁCS, B. (2014) The duality of organizations and audiences. *Anal. Sociol.*, 397–418.
36. LOMI, A. & PALLOTTI, F. (2012) Relational collaboration among spatial multipoint competitors. *Soc. Netw.*, **34**, 101–111.
37. ROBINS, G. & ALEXANDER, M. (2004) Small worlds among interlocking directors: network structure and distance in bipartite graphs. *Comput. Math. Organ. Theory*, **10**, 69–94.
38. VALEEEVA, D., HEEMSKERK, E. M. & TAKES, F. W. (2020) The duality of firms and directors in board interlock networks: a relational event modeling approach. *Soc. Netw.*, **62**, 68–79.
39. UZZI, B. & SPIRO, J. (2005) Collaboration and creativity: the small world problem. *Am. J. Sociol.*, **111**, 447–504.
40. LERNER, J. & LOMI, A. (2019) Team diversity, polarization, and productivity in online peer production. *Soc. Netw. Anal. Mining*, **9**, 1–17.
41. EVERETT, M. G. & BORGATTI, S. P. (2013) The dual-projection approach for two-mode networks. *Soc. Netw.*, **35**, 204–210.
42. ROBERTS JR, J. M. (2000) Correspondence analysis of two-mode network data. *Soc. Netw.*, **22**, 65–72.
43. FREEMAN, L. C. & WHITE, D. R. (1993) Using Galois lattices to represent network data. *Sociol. Methodol.*, 127–146.
44. MCPHERSON, J. M. (1982) Hypernetwork sampling: duality and differentiation among voluntary organizations. *Soc. Netw.*, **3**, 225–249.

45. EVERETT, M. G. & BORGATTI, S. P. (1993) An extension of regular colouring of graphs to digraphs, networks and hypergraphs. *Soc. Netw.*, **15**, 237–254.
46. SEIDMAN, S. B. (1981) Structures induced by collections of subsets: a hypergraph approach. *Math. Soc. Sci.*, **1**, 381–396.
47. KOSKINEN, J. & EDLING, C. (2012) Modelling the evolution of a bipartite network—peer referral in interlocking directorates. *Soc. Netw.*, **34**, 309–322.
48. SNIJders, T. A., LOMI, A. & TORLÓ, V. J. (2013) A model for the multiplex dynamics of two-mode and one-mode networks, with an application to employment preference, friendship, and advice. *Soc. Netw.*, **35**, 265–276.
49. ABBOTT, A. (1997) Of time and space: the contemporary relevance of the Chicago School. *Soc. forces*, **75**, 1149–1182.
50. FELD, S. L. (1981) The focused organization of social ties. *Am. J. Sociol.*, **86**, 1015–1035.
51. CHODROW, P. & MELLOR, A. (2020) Annotated hypergraphs: models and applications. *Appl. Netw. Sci.*, **5**, 9.
52. CONALDI, G., LOMI, A. & TONELLATO, M. (2012) Dynamic models of affiliation and the network structure of problem solving in an open source software project. *Organ. Res. Methods*, **15**, 385–412.
53. KRIVITSKY, P. N. & HANDCOCK, M. S. (2014) A separable model for dynamic networks. *J. R. Stat. Soc. B*, **76**, 29–46.
54. WANG, P., PATTISON, P. & ROBINS, G. (2013) Exponential random graph model specifications for bipartite networks—a dependence hierarchy. *Soc. Netw.*, **35**, 211–222.
55. HOFFMAN, M., BLOCK, P., ELMER, T. & STADTFELD, C. (2020) A model for the dynamics of face-to-face interactions in social groups. *Netw. Sci.*, 1–22.
56. LERNER, J. & LOMI, A. (2020b) Reliability of relational event model estimates under sampling: how to fit a relational event model to 360 million dyadic events. *Netw. Sci.*, **8**, 97–135.
57. LOMI, A., MASCIA, D., VU, D. Q., PALLOTTI, F., CONALDI, G. & IWASHYNA, T. J. (2014) Quality of care and interhospital collaboration: a study of patient transfers in Italy. *Med. Care*, **52**, 407.
58. BRESLOW, N. (1974) Covariance analysis of censored survival data. *Biometrics*, 89–99.
59. HERTZ-PICCIOTTO, I. & ROCKHILL, B. (1997) Validity and efficiency of approximation methods for tied survival times in Cox regression. *Biometrics*, 1151–1156.
60. PRENTICE, R. L. & KALBFLEISCH, J. D. (1979) Hazard rate models with covariates. *Biometrics*, 25–39.
61. DUBoIS, C., BUTTS, C. T., McFARLAND, D. & SMYTH, P. (2013) Hierarchical models for relational event sequences. *J. Math. Psychol.*, **57**, 297–309.
62. GIBSON, D. R. (2005) Taking turns and talking ties: networks and conversational interaction. *Am. J. Sociol.*, **110**, 1561–1597.
63. KIM, B., SCHEIN, A., DESMARAIS, B. A. & WALLACH, H. (2018) The hyperedge event model. *arXiv preprint arXiv:1807.08225*.
64. AALEN, O., BORGAN, O. & GJESSING, H. (2008) *Survival and Event History Analysis: A Process Point of View*. Springer Science & Business Media.
65. COX, D. (1972) Regression models and life-tables. *J. R. Stat. Soc. B (Methodological)*, **34**, 87–22.
66. THERNEAU, T. M. & GRAMBSCH, P. M. (2013) *Modeling Survival Data: Extending the Cox Model*. Springer Science & Business Media.
67. BORGAN, Ø., GOLDSTEIN, L. & LANGHOLZ, B. (1995) Methods for the analysis of sampled cohort data in the Cox proportional hazards model. *Ann. Stat.*, 1749–1778.
68. KEOGH, R. H. & COX, D. R. (2014) *Nested Case–Control Studies*, chapter 7. Institute of Mathematical Statistics Monographs. Cambridge University Press, pp. 160–190.
69. BARABÁSI, A.-L. & ALBERT, R. (1999) Emergence of scaling in random networks. *Science*, **286**, 509–512.
70. ROBINS, G., PATTISON, P. & WANG, P. (2009) Closure, connectivity and degree distributions: exponential random graph (p^*) models for directed social networks. *Soc. Netw.*, **31**, 105–117.
71. HEIDER, F. (1946) Attitudes and cognitive organization. *J. Psychol.*, **21**, 107–112.
72. BURT, R. S. (1992) *Structural Holes: The Social Structure of Competition*. Harvard University Press.
73. BRANDES, U. & PICH, C. (2008) An experimental study on distance-based graph drawing. *International Symposium on Graph Drawing* (I. G. Tollis & M. Patrignani eds). Springer, pp. 218–229.

74. BRANDES, U. & MADER, M. (2011) A quantitative comparison of stress-minimization approaches for offline dynamic graph drawing. *International Symposium on Graph Drawing* (M. van Kreveld & B. Speckmann eds). Springer, pp. 99–110.
75. BAUR, M., BENKERT, M., BRANDES, U., CORNELSEN, S., GAERTLER, M., KÖPF, B., LERNER, J. & WAGNER, D. (2001) Visone Software for visual social network analysis. *International Symposium on Graph Drawing* (P. Mutzel, M. Jünger, & S. Leipert eds). Springer, pp. 463–464.
76. LERNER, J., INDLEKOFER, N., NICK, B. & BRANDES, U. (2013) Conditional independence in dynamic networks. *J. Math. Psychol.*, **57**, 275–283.
77. CARNWELL, B. (2015) *Social Sequence Analysis: Methods and Applications*, vol. 37. Cambridge University Press.
78. HOMANS, G. C. (1950) *The Human Group*. Taylor and Francis Group.
79. MOHR, J. W. & WHITE, H. C. (2008) How to model an institution. *Theory Soc.*, **37**, 485–512.